

Ionospheric TEC Disturbances over South Korea Following the 2011 Great Tohoku Earthquake

¹Byung-Kyu Choi, ²Sang Jeong Lee, ³Ha Su Yoon

^{1,3}Space Geodesy Group, Space Science Division, Korea Astronomy and Space Science Institute (KASI)

²Department of Electronics Engineering, Chungnam National University

Abstract: Ionospheric total electron contents (TEC) disturbances following the 2011 great Tohoku earthquake on March 11, 2011 were observed by a GPS network in South Korea. The impulsive TEC enhancements were first observed approximately 16.5 minutes after the beginning of the earthquake. Various types of seismic waves were also observed over South Korea. To investigate more detailed disturbances in the TEC, we processed the GPS data with a sampling rate of 1Hz and applied a band-pass filter with corner frequencies of 0.0 and 0.005 Hz. Small-scale traveling ionospheric disturbances (TIDs) with a period of approximately 4 minutes (~250 seconds) were observed from 6:15 to 7:10 UT. These variations are considered to be a clear manifestation of the acoustic resonance oscillations. We also observed medium-scale TIDs with a period of approximately 15 minutes and a duration of approximately 60 minutes. A remarkable finding is that the damping of the amplitude of the medium-scale TIDs was observed clearly in the time series.

Keywords: ionosphere; earthquake; TEC; disturbance.

I. Introduction

Sudden ionospheric disturbances can be caused by a variety of factors, including solar flares, geomagnetic storms, space weather and seismic events. Various studies of disturbances of the ionospheric total electron content (TEC) following seismic events have been conducted with the global positioning system (GPS) have been investigated for two decades (Heki and Ping, 2005; Otsuka *et al.*, 2006, Choosakulet *et al.*, 2009). Heki and Ping (2005) showed directivity and clear velocity of the coseismic ionospheric disturbance (CID) triggered by the 2003 Tokachi-Oki earthquake (Mw 8.0) with a GPS network in Japan. Otsuka *et al.* (2006) detected ionospheric TEC enhancements induced by large earthquakes. Their report was based on GPS data from Indonesia and Thailand. They also found the enhancement of ionospheric TEC on the northwards of the epicenter with cycles of 14 to 40 minutes after the 2004 Sumatra-Andaman earthquake. In particular, Choosakul *et al.* (2009) reported a periodic oscillation of ionospheric TEC measured by a GPS network following the 2004 Sumatra earthquake. It lasted for more than three hours in the vicinity of the epicenter and had an obvious periodicity at 3.7 mHz and 4.4 mHz.

Recently, a massive earthquake with a magnitude of 9.0 occurred in the Tohoku area, on the east coast of Honshu, Japan (38.322°N, 142.369°E, depth 32km) at 05:46:23 UT (universal time) on 11 March 2011. The ionospheric disturbances generated by this large earthquake and tsunami have been analyzed by many investigators (Maruyama *et al.*, 2011; Matsumura *et al.*, 2011; Saito *et al.*, 2011; Tsugawa *et al.*, 2011; Tsai *et al.*, 2001; Liu *et al.*, 2011; Rolland *et al.*, 2011). Maruyama *et al.* (2011) observed ionospheric disturbances in ionograms obtained at the four ionosondes in Japan. Matsumura *et al.* (2011) reported that ionospheric TEC oscillations induced by the Tohoku earthquake show a good agreement with simulated atmospheric perturbations. This result indicates that ionospheric oscillations are associated with the motion of the neutral atmosphere. Saito *et al.* (2011) revealed that a displacement of the sea surface caused by the earthquake induced atmospheric waves, which propagated upwards to the thermosphere. Tsugawa *et al.* (2011) detected ionospheric TEC disturbances following the Tohoku earthquake with a dense GPS network in Japan. They calculated the vertical TEC from data recorded at a GPS station and also found that the sudden depletions of the TEC and the short-period oscillations after the earthquake were observed in the signals of some GPS satellites. Tsai *et al.* (2011) studied the ionospheric signature induced by the Tohoku earthquake with a network of several GPS facilities, including GEONET in Japan, 7 IGS sites, and Taiwan stations. These authors indicated that the ionospheric perturbations are primarily produced by the earthquake. Liu *et al.* (2011) observed remarkable signatures, including Rayleigh waves, acoustic gravity waves, and tsunami waves triggered by the M9.0 Tohoku earthquake. These phenomena were observed from the ground-based GPS networks in Japan and Taiwan. Rolland *et al.* (2011) analyzed the ionosphere TEC variations associated with the Tohoku earthquake. They also observed three different types of wave: the Rayleigh surface waves, acoustic waves and gravity waves. These observations show good agreement with the observations of Liu *et al.* (2011).

GPS data can be used to observe the ionospheric disturbances recorded following large earthquakes. Ground-based GPS data allow the detection of anomalies in the ionospheric TEC. In this paper, we processed GPS

data from 9 ground-based GPS reference stations in the Korean GPS network (KGN) to detect various types of the ionospheric TEC disturbances induced by the 2011 great Tohoku earthquake.

This paper also focuses on a detailed investigation of a periodic oscillation and the high-resolution observation of the TEC disturbances induced by the Tohoku earthquake. For this purpose, we used GPS data with two different sampling parameters: a sampling interval of 30 sec and a sampling rate of 1Hz.

II. GPS Data And Method

To investigate ionospheric disturbances over South Korea following the Tohoku earthquake, we processed the GPS data obtained from the KGN in South Korea (9 GPS stations designated as ‘daej’, ‘bhao’, ‘jeju’, ‘kohg’, ‘mlyn’, ‘mkpo’, ‘sbao’, ‘skch’ and ‘skma’). The estimation methods used to extract TEC information from GPS signals have been described by several investigators (Klobuchar *et al.*, 1994; Klobuchar, 1996; Jakowski *et al.*, 1996).

The fundamental equations for the code and carrier phase measurements can be expressed as follows (Schaer, 1999).

$$P = \rho + c \cdot (dt^s - dt_r) + c \cdot (d^s + d_r) + d_{ion} + d_{trop} + \varepsilon_p \quad (1)$$

$$\Phi = \rho + c \cdot (dt^s - dt_r) - d_{ion} + d_{trop} + \lambda \cdot N + \varepsilon_\Phi \quad (2)$$

Where,

- ρ true geometric range from satellite to receiver (m)
- dt^s satellite clock error (s)
- dt_r receiver clock error (s)
- d^s satellite hardware bias (s)
- d_r receiver hardware bias (s)
- c speed of light in a vacuum (m/s)
- d_{ion} ionospheric delay (m)
- d_{trop} tropospheric delay (m)
- λ wavelength of frequency (m)
- N carrier phase integer ambiguity (cycle)
- ε measurement noises (m)

The estimated TEC values derived from the code measurements have a large uncertainty due to the high noise. The carrier phase measurements are much more accurate than the code measurements, but carrier phase measurements require the resolution of phase ambiguity and consideration of infrequent cycle slips. To obtain better accuracy for the derived GPS-TEC, a smoothing technique is employed with the code and carrier phase measurements. The smoothed code with the carrier phase is described as follows:

$$P(t)_{sm} = \omega \cdot P(t) + (1 - \omega) \cdot \{P(t-1)_{sm} + \lambda \cdot (\Phi(t) - \Phi(t-1))\} \quad (3)$$

Where $P(t)$ and $\Phi(t)$ are the pseudo-range and carrier phase measurements. The term ω is the smoothing factor. The term $P(t)_{sm}$ is the smoothed code. To calculate the ionospheric TEC, we adopted the common model in which the ionosphere consists of a thin shell at a fixed height, usually 350 km. Slant TEC is a measure of the total electron content of the ionosphere along the ray path. It can be easily computed from the following Eq.(4).

$$STEC = \frac{1}{40.3} \left(\frac{f_1^2 \cdot f_2^2}{f_1^2 - f_2^2} \right) (P_2 - P_1 + D^s + D_r) \quad (4)$$

Where, $D^s = d_2^s - d_1^s$ and $D_r = d_{2r} - d_{1r}$, are the differential code bias (DCB) of the satellite and the receiver, respectively. It is well known that these biases significantly affect the ionospheric TEC value (Ma and Maruyama, 2003; Choi *et al.*, 2011). The DCB values were obtained with weighted least squares and applied to the daily averaged estimates.

In this study, we obtained TEC values from ground-based GPS data with a 30 second sampling interval. In addition, we processed GPS data with a 1Hz sampling rate from the ‘daej’ GPS station to allow more detailed investigation of the TEC disturbances. The time-differenced vertical TEC for each GPS receiver-satellite pair was considered to reveal the variation in the TEC due to the earthquake and the tsunami. To enhance the coherence of the characteristics of seismic-wave propagation, a band-pass filter was also applied to the TEC time series.

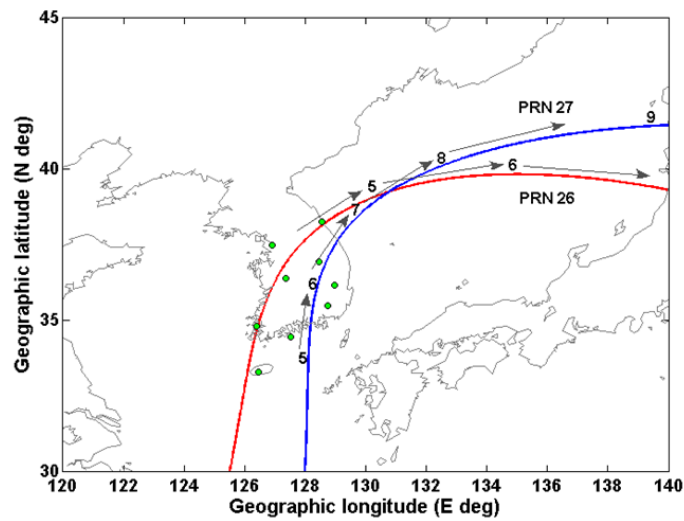


Figure 1 The locations of 9 GPS reference stations in South Korea (green dots). The IPPs for the PRN 26 (red line) and PRN 27 (blue line) satellite-receiver pairs on March 11, 2011. The digits represent the corresponding UT hours.

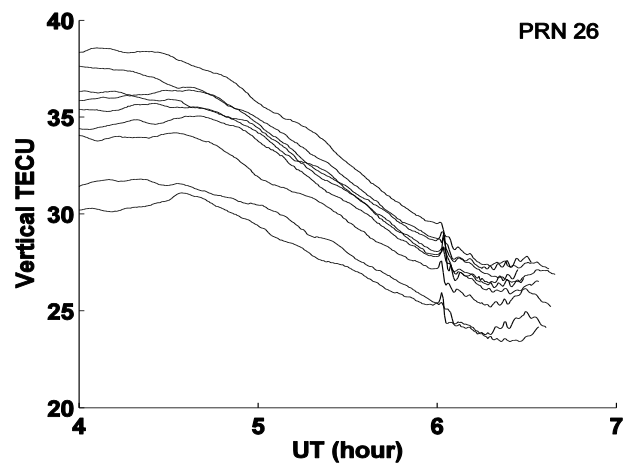


Figure 2 The vertical TEC variations of the PRN 26 satellite observed from 9 GPS stations in South Korea on March 11, 2011.

III. Results

To study the ionospheric disturbances over South Korea following the 2011 Tohoku earthquake, we processed GPS data from the KGN in South Korea.

Figure 1 shows the IPPs for the PRN 26 and PRN 27 satellites. The IPPs for the PRN 26 satellite are approaching the epicenter across the Korean Peninsula. The IPPs for the PRN 27 satellite resemble those of PRN 26. They remained in the vicinity of South Korea for almost three hours after the onset of the earthquake. The digits represent the corresponding time.

Figure 2 shows the time series of the vertical TEC of the PRN 26 satellite observed by 9 GPS reference stations in South Korea. The vertical TEC estimated from all GPS sites showed impulsive enhancements with amplitudes of 0.5~1 TECU at 06:02 UT. After the impulsive TEC enhancements, sudden decreases in the vertical TEC were observed. Compared with the TEC before the impulsive enhancements, the average amplitude of the TEC decreases was approximately 1 TECU. Small-scale TEC perturbations, weaker than 0.5 TECU, appeared during short periods from 06:00 UT to 06:30 UT. Tsugawa *et al.* (2011) reported a decrease of 20% in the TEC measurements relative to the previous TEC value (before the depletions occurred) over Japan.

Figure 3 represents the time series of the time-differenced vertical TEC (TECU/30sec) of the PRN 26 satellite at 9 GPS stations. We considered the distance from the GPS stations to the epicenter. The ‘bhae’ station in South Korea was closest to the epicenter and the ‘jeju’ station was the farthest from the epicenter. The

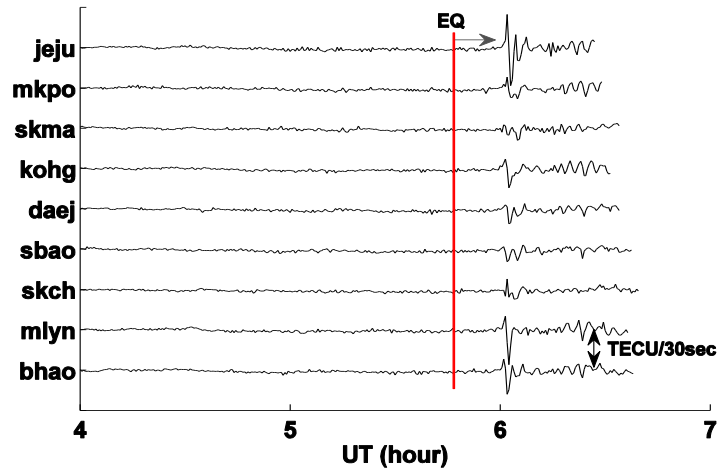


Figure 3 The time-differenced vertical TEC of the PRN 26 satellite at 9 GPS stations on March 11, 2011. The y-axis shows the 4 characters used to represent the site name. The red line indicates the beginning of the earthquake.

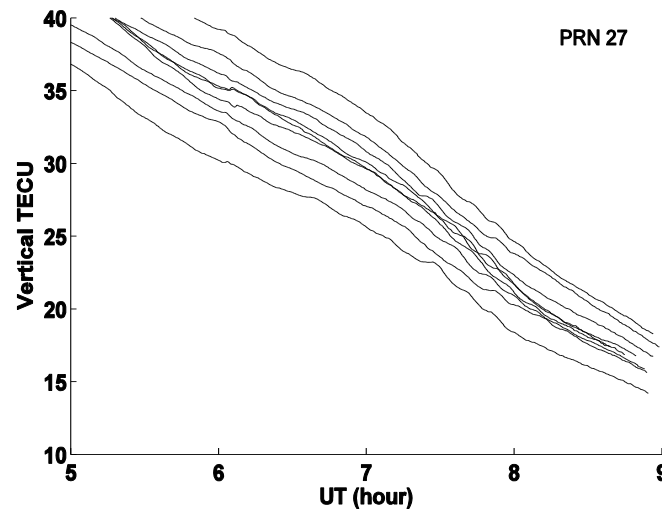


Figure 4 The vertical TEC variations of the PRN 27 satellite observed from 9 GPS stations in South Korea on March 11, 2011.

behaviours of the time-differenced TEC (TEC/30 sec) before the earthquake were very quiet. No remarkable variations in the TEC were observed over South Korea for approximately 16 minutes after the earthquake. Irregular fluctuations in the TEC were first observed at 06:02 UT over almost all of South Korea. However, few time differences in the arrival of the disturbances were observed. It is known that the seismic perturbations triggered by the earthquake affected the ionospheric TEC over South Korea. Liu *et al.* (2011) reported that these perturbations are described as seismo-traveling ionospheric disturbances (STIDs). A remarkable finding is that the impulsive variations in the TEC estimated by the 'jeju' station were relatively higher than those estimated by the other stations. This difference could be associated with the direction of propagation of the first large-scale circular waves triggered by the earthquake. According to Heki and Ping (2005), a CID is only detected in a magnetic equatorward direction due to magnetic field inclination. Tohoku earthquake observations showed clear north-south asymmetry of the CID excited by the Rayleigh wave (Yoshiho *et al.*, 2013). Therefore our result is related to an asymmetry of the CID.

Figure 4 shows the time series of the vertical TEC of the PRN 27 satellite observed by 9 GPS stations from 05:00 UT to 09:00 UT. The TEC variations showed no remarkable features before 07:15 UT. Weak fluctuations in the TEC variations with a period of approximately 15 min were just observable from 07:15 to 08:15 UT. These fluctuations were identified as the slower CID propagated in all direction from the tsunami source.

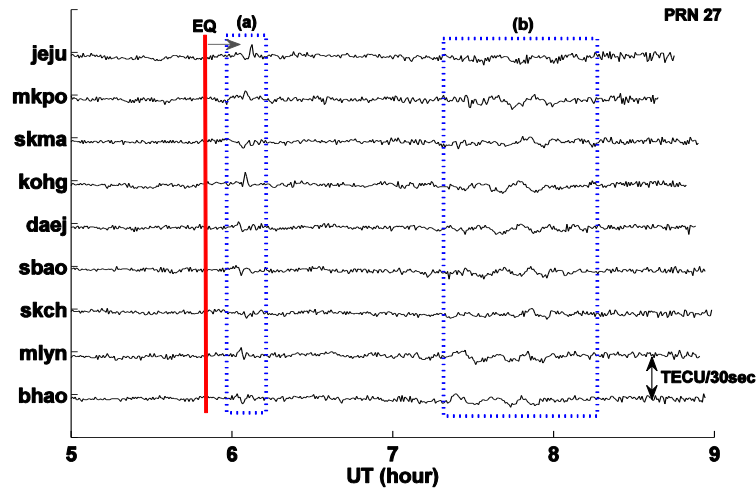


Figure 5 The time-differenced vertical TEC of the PRN 27 satellite at 9 GPS stations on March 11, 2011. The y-axis shows the 4 characters used to represent the site name.

Figure 5 shows the time series of the time-differenced vertical TEC (TEC/30 sec) of the PRN 27 satellite. As shown in Figure 5(a), the initial ionospheric TEC disturbances appeared at 06:02 UT. The absolute amplitude of the TEC variations in the short period was approximately 0.3 TEC. Following the impulsive perturbations, no further features of the TEC variations were observed until 07:15 UT. However, remarkable small TEC fluctuations, not shown by Figure 6, were observed after 07:15 UT all over South Korea. As shown in Figure 5(b), our results indicate that regular wave patterns in the TEC variations were clearly observed for one hour from 07:15 UT to 08:15 UT. These waves, shown in Figure 5(b), also exhibited repeated short-period oscillation over a period of one hour.

Tsugawa *et al.* (2011) reported that medium-scale concentric waves with a wavelength of 200-300 km were observed until after 08:00 UT in western Japan after the propagation of the first large-scale circular waves triggered by the Tohoku earthquake. Our findings are in good agreement with this result.

To investigate more detailed variations in the TEC over South Korea following the Tohoku earthquake, we processed the GPS data with a sampling rate of 1 Hz obtained from the ‘daej’ station and examined the temporal variation of the TEC data. A band-pass filter with corner frequencies of 0.0 and 0.005 Hz was also applied to enhance the coherence of the characteristics of seismic-wave propagation.

Figure 6 shows the TEC time series for satellite 26 at the ‘daej’ station in South Korea. The behavior of the vertical TEC decreased linearly approximately 15 minutes after the beginning of the earthquake. A small impulsive enhancement with an amplitude of 0.3 TEC then occurred at 06:02 UT. Following the impulsive enhancement, the TEC showed rapid decreases until 06:07 UT. The amount of the depletion of TEC was approximately 1.3 TECU relative to the TEC before the impulsive enhancement. The lower image in Figure 6 shows the time series of the time-differenced TEC ($dTEC = TEC/1sec$). The blue dotted line in Figure 6 represents the time series of the dTEC obtained from 1 Hz data at the ‘daej’ GPS station. The amplitude of the time-differenced TEC for the PRN 26 satellite showed a maximum of ~ 0.03 TEC. From these results, we do not observe coseismic signatures clearly. However, the application of a band-pass filter to the TEC variations allowed us to observe the features in TEC fluctuations induced by the earthquake. The red line in Figure 6 represents the time series of the band-pass filtered TEC variations. The sudden disturbances of the TEC variations at 06:02 UT are assumed to result from the main shock produced by the earthquake. After the main shock, small-scale periodic oscillation with a period of about 4 minutes was observed continuously. It is explained that an acoustic wave triggered by a propagating Rayleigh wave shows an atmospheric resonance.

We could also observe remarkable features of the TEC variations for a longer time, as shown in Figure 7. Figure 7 presents the time series of the band-pass filtered TEC variations from the PRN 27 satellite. We observed two types of perturbations in the TEC variations following the Tohoku earthquake. Sudden disturbances in the TEC variations are clearly visible at 06:02 UT. Small amplitude TEC variations were observed from 6:15 to 7:15 UT. We detected variations in TEC with a time period of approximately 4 minutes (~ 250 seconds) and a duration of approximately 1 hour. To calculate a period of the oscillation, an averaging time of the consecutive peak-to-peak amplitude was used. The period was kept constant. These variations are considered to represent a clear instance of the acoustic waves. Using 1 Hz sampling TEC data, we have found that the short-period oscillations (4 minutes) caused by the acoustic resonance are detected continuously for one

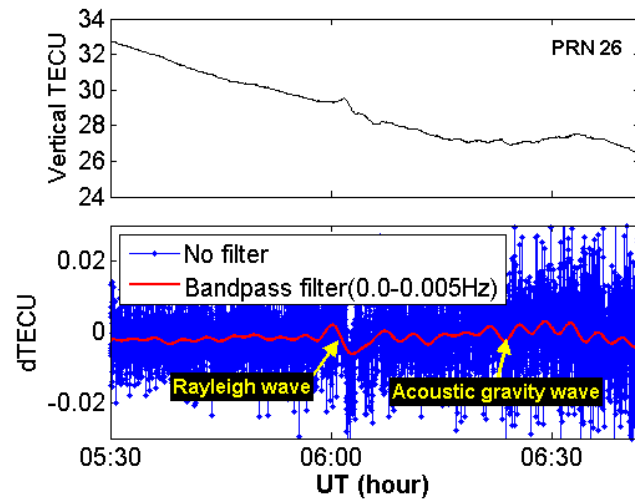


Figure 6 TEC time series for satellite 26 calculated with high-resolution GPS data (the sampling rate is 1Hz) from 05:30-06:45 UT. The upper panel represents the TEC time series. The lower panel represents the time series of the corresponding TEC variations. The red line represents the band-pass filtered TEC variations, analyzed using corner frequencies of 0.0 and 0.005 Hz.

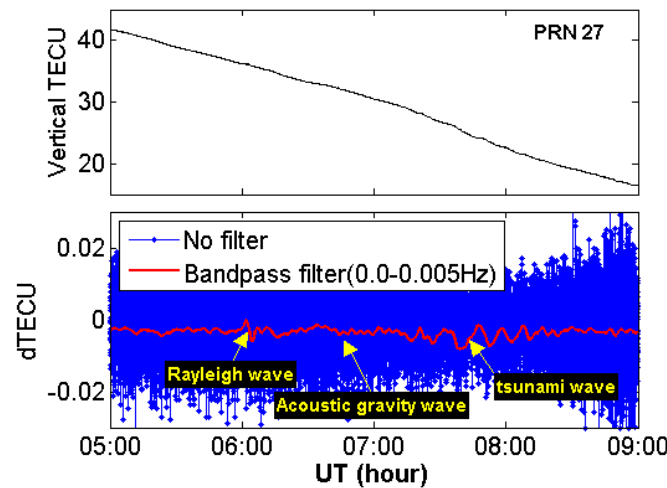


Figure 7 TEC time series of satellite 27 calculated with the GPS data with a sampling rate of 1 Hz from 05:00-09:00 UT. The upper panel represents the TEC time series. The lower panel represents the time series of the corresponding TEC variations. The red line represents the band-pass filtered TEC variations.

hours over South Korea. These TEC responses agreed with the results of earlier studies (Calais and Minster, 1995; Afraimovich *et al.*, 2006). Moreover, we observed medium-scale TIDs with a period of 15 minutes and a duration of 60 minutes. These perturbation structures appeared at approximately 07:30 UT and gradually disappeared after 08:30 UT. They formed intensive quasi-periodic TEC variations. An interesting feature of these structures is that the amplitude of medium-scale TIDs was clearly observed on the time series. The amplitude of wave showed a gradual decrease. After 8:30 UT, the amplitude became small. This is coincident with the report by Saito *et al.* (2011). The amplitude change would be generated by the coupling of acoustic resonance between the ground surface and the lower thermosphere. Further detailed analysis is necessary to discuss the relationship between the amplitude change and the TEC variations. The GPS data with a 1 Hz sampling rate enables us to obtain detailed observations of the propagation and attenuation of medium-scale TIDs. Such ionospheric disturbances were observed for four hours at the northwest of the epicenter, to the east of South Korea.

IV. Discussion And Summary

Ionospheric TEC disturbances induced by the 2011 Tohoku earthquake on March 11, 2011 were investigated using a GPS network in South Korea. Impulsive TEC enhancements were first observed

approximately 16.5 minutes after the beginning of the earthquake. The CID associated with the Rayleigh wave was observed in west direction (over South Korea) from the epicenter. Astafyeva and Heki (2009) explained that the shape of the response depends on the location of sub-ionospheric points (SIPs) relative to the epicenter. In our results, the amplitude of the waves reached the maximum value of 0.9 TEC at the 'jeju' station and then decreased to 0.1-0.2 TEC. The SIPs recorded from the GPS stations in South Korea are located approximately 1,250 km away from the ionospheric epicenter. The CID propagated with the velocity 1.26 km/s from the epicenter to South Korea. If it is assumed that the STIDs induced on the Earth's surface reach the ionosphere at approximately 05:53 UT, the wave speed is 2.31 km/s (1250 km/540 seconds), which is within the range of Rayleigh surface wave speeds. These features are also consistent with previous observations (Astafyeva *et al.*, 2009; Rolland *et al.*, 2011).

Short-period TEC oscillations were observed more than one hour over South Korea after the earthquake. Tsugawa *et al.* (2011) reported that medium-scale concentric waves were observed until after 08:30 UT in western Japan. Large earthquakes can generate acoustic waves and gravity waves which propagate into the ionosphere and interact with the ionized gases. The oscillation of seismic waves such as Rayleigh waves, acoustic waves, gravity waves and tsunami waves triggered by Tohoku earthquake continued for four hours above the epicenter. This implies that the resonance of the acoustic waves was lasted for four hours after earthquake onset.

To investigate more detailed features of the TEC perturbations, the GPS data from the 'daejeon' site with a sampling rate of 1 Hz were processed. We observed clear features of small-scale and medium-scale waves in the TEC variations in the time series, as shown in Figure 6 and 7. In Figure 6, we could observe signatures of Rayleigh surface waves and the acoustic gravity waves. The distance of the SIPs of the PRN 26 satellite and the ionospheric epicenter was approximately 510 km. Therefore the velocity of wave can be easily calculated using time difference in any direction. Its wave speed was about 1.05 km/s. Heki and Ping (2005) showed that the acoustic wave speed is about 0.6-1.1 km/s at 300 km altitude in the ionosphere. Using numerical simulations, Matsumura *et al.* (2011) indicated that the atmospheric waves were generated by a sea surface displacement induced from the large earthquake, not by a propagating tsunami.

As shown in Figure 7, the acoustic waves with a period of approximately 250 seconds (about 4 minutes) and a duration of approximately 60 minutes were the first detailed aspects of the TEC variations found in 1 Hz TEC data. They are considered to represent a manifestation of the acoustic resonance oscillations. These waves were not seen in 30 seconds data.

We also observed medium-scale TIDs with a period of approximately 15 minutes and a duration of one hour. These medium-scale TIDs structures appeared at approximately 07:30 UT over eastern South Korea. The amplitude of the medium-scale waves tended to decrease with time. It is assumed that these waves are induced by the tsunami due to the slow speed. These waves propagated for more than horizontal distance of 1,000 km from the ionospheric epicenter.

The use of the GPS data with a 1 Hz sampling rate enabled us to observe clearly the seismic waves expanding as far as horizontal distance of 1,000 km from the epicenter. This approach also enabled us to observe the details of the propagation and attenuation of the acoustic wave over South Korea.

References

- [1]. Afraimovich, E.L., Astafieva, E.I., Kirushkin, V.V. Localization of the source of ionospheric disturbance generated during an earthquake. *Int. J. Geomagn. Aeron.*, 6, G12002, doi:10.1029/2004GI000092, 2006.
- [2]. Astafyeva, E., Heki, K. Dependence of waveform of near-field coseismic ionospheric disturbances on focal mechanisms. *Earth Planets Space.*, 61, 939-943, 2009.
- [3]. Astafyeva, E., Heki, K., Kiryushkin, V., Afraimovich, E., Shalimov, S. Two-mode long-distance propagation of coseismic ionosphere disturbances. *J. Geophys. Res.*, 114, doi:10.1029/2008JA013853, 2009.
- [4]. Calais, E., Minster, J.B. GPS detection of ionospheric perturbations following the January 17, 1994, Northridge earthquake. *Geophys. Res. Lett.*, 22, 1045-1048, 1995.
- [5]. Chen, C.H., Saito, A., Lin, C.H., Liu, J.Y., Tsai, H.F., Tsugawa, T., Otsuka, Y., Nishioka, M., Matsumura, M. Long-distance propagation of ionospheric disturbance generated by the 2011 off the Pacific coast of Tohoku Earthquake. *Earth Planets Space*, 63, 881-884, 2011.
- [6]. Choi, B.K., Cho, J.H., Lee, S.J. Estimation and analysis of GPS receiver differential code biases using KGN in Korean Peninsula. *Adv. in Space Res.*, 47, 1590-1599, 2011.
- [7]. Choosakul, N., Saito, A., Iyemori, T., Hashizume, M. Excitation of 4-min periodic ionospheric variations following the great Sumatra-Andaman earthquake in 2004. *J. Geophys. Res.*, 114, A10313, doi:10.1029/2008JA013915, 2009.
- [8]. Grejner-Brzezinska, D., Wielgosz, P., Kashni, I., Smith, D.A., Spencer, P., Robertson, S., Mader, G.L. An analysis of the effects of different network-based ionosphere estimation models on rover positioning accuracy. *J. GPS.*, 3, 115-131, 2004.
- [9]. Heki, K., Ping, J.S. Directivity and apparent velocity of the coseismic ionospheric disturbances observed with a dense GPS array. *Earth Planet. Sci. Lett.*, 236, 845-855, 2005.
- [10]. Jakowski, N., Schlüter, S., Sardon, E. Total electron content of the ionosphere during the geomagnetic storm on 10 January 1997. *J. Atmos. Sol. Terr. Phys.*, 61, 299-307, 1999.
- [11]. Klobuchar, J.A. Ionospheric Effects on GPS, in *Global Positioning Systems: Theory and Applications*, Vol. I, Proc. in Astronaut. and Aeronaut., edited by Parkinson, B.W., Spilker, J.J., American Institute of Aeronautics and Astronautics, Washington, 485-515, 1996.

- [12]. Klobuchar, J.A., Doherty, P.H., Bailey, G.J., Davies, K. Limitations in determining absolute total electron content from dual-frequency GPS group delay measurements. In: Kersley, L. (Ed). *Proceedings of the International Beacon Satellite Symposium*, Aberystwyth, UK, 1-4, 1994.
- [13]. Liu, J.Y., Tsai, H.F., Lin, C.H., Kamogawa, M., Chen, Y.I., Lin, C.H., Huang, B.S., Yu S.B., Yeh, Y.H. Coseismic ionospheric disturbances triggered by the Chi-Chi earthquake. *J. Geophys. Res.*, 115, A08303, 2010.
- [14]. Liu, J.Y., Chen, C.H., Lin, C.H., Tsai, H.F., Chen, C.H., Kamogawa, M. Ionospheric disturbances triggered by the 11 March 2011 M9.0 Tohoku earthquake. *J. Geophys. Res.*, 116, A06319, doi:10.1029/2011JA016761, 2011.
- [15]. Ma, G., Maruyama, T. Derivation of TEC and estimation of instrumental biases from GEONET in Japan. *Ann. Geophys.*, 21, 2083-2093, 2003.
- [16]. Maruyama, T., Tsugawa, T., Kato, H., Saito, A., Otsuka, Y., Nishioka, M. Ionospheric multiple stratifications and irregularities induced by the 2011 off the Pacific coast of Tohoku Earthquake. *Earth Planets Space*, 63, 869-873, 2011.
- [17]. Matsumura, M., Saito, A., Iyemori, T., Shinagawa, H., Tsugawa, T., Otsuka, Y., Nishioka, M., Chen, C.H. Numerical simulations of atmospheric waves excited by the 2011 off the Pacific coast of Tohoku Earthquake. *Earth Planets Space*, 63, 885-889, 2011.
- [18]. Otsuka, Y., Kotake, N., Tsugawa, T., Shiokawa, K., Ogawa, T., Effendy, Saito, S., Kawamura, M., Maruyama, T., Hemmakorn, N., Komolmis, T. GPS detection of total electron content variations over Indonesia and Thailand following the 26 December 2004 earthquake. *Earth Planets Space*, 58, 159-165, 2006.
- [19]. Rolland, L.M., Lognonne, P., Astafyeva, E., Kherani, E.A., Kobayashi, N., Mann, M., Munekane, H. The resonant response of the ionosphere imaged after the 2011 off the Pacific coast of Tohoku Earthquake. *Earth Planets Space Lett.*, 63, 853-857, 2011.
- [20]. Saito, A., Tsugawa, T., Otsuka, Y., Nishioka, M., Iyemori, T., Matsumura, M., Saito, S., Chen, C.H., Goi, Y., Choosakul, N. Acoustic resonance and plasma depletion detected by GPS total electron content observation after the 2011 off the Pacific coast of Tohoku Earthquake. *Earth Planets Space*, 63, 863-867, 2011.
- [21]. Schaer, S., *Mapping and Predicting the Earth's Ionosphere Using the Global Positioning System*, Ph.D. thesis, University of Berne, Switzerland, 1999.
- [22]. Tsai, H.F., Liu, J.Y., Liu, C.H., Chen, C.H. Tracking the epicenter and the tsunami origin with GPS ionosphere observation. *Earth Planets Space*, 63, 859-863, 2011.
- [23]. Tsugawa, T., Saito, A., Otsuka, Y., Nishioka, M., Maruyama, T., Kato, H., Nagatsuma, T., Murata, K.T. Ionospheric disturbances detected by GPS total electron content observation after the 2011 off the Pacific coast of Tohoku Earthquake. *Earth Planets Space*, 63, 875-879, 2011.
- [24]. Yoshihiro, K., Masashi, K., Shigeto, W., Masatsugu, O., Toru, M., Liu, J.Y., Sun, Y.Y., Takuji, Y. Ionospheric ripples excited by superimposed wave fronts associated with Rayleigh waves in the thermosphere. *J. Geophys. Res.*, 118, doi:10.1002/jgra.50099, 2013.